Distributed Detection in Millimeter Wave Massive MIMO Wireless Sensor Networks

***Abstract*—This paper considers a distributed detection framework for millimeter wave (mmWave) massive multiple-input multiple-output (MIMO) wireless sensor networks (WSNs). A hybrid combining based low complexity fusion rule is derived at the fusion center (FC) that also incorporates the local probabilities of detection and false alarm of the individual sensor nodes, thus making it suitable for practical scenarios. Closed-form expressions are obtained for the probabilities of detection and false alarm are evaluated to characterize the system performance. Moreover, a deflection coefficient maximization based framework is also developed to determine the signaling matrix that further improves the detection performance of the proposed scheme. Finally, simulation results are presented to demonstrate the performance of the proposed detector and to corroborate the analytical results.**

I. Introduction

Millimeter wave (mmWave) communication, which exploits the spectrum in the 30 GHz to 300 GHz band, has shown excellent potential toward enabling high data rates in next-generation 5G communication systems [1]. However, mmWave communication faces several challenges, such as higher path losses, severe signal blockage and increased hardware complexity when compared to conventional systems operating at carrier frequencies below 6 GHz [2]. In this context, massive multiple-input multiple-output (MIMO) technology, which can provide both antenna directivity and array gains, can be employed to compensate for the increased propagation losses experienced at mmWave frequencies. Therefore, the integration of mmWave and massive MIMO technologies leads to the ability to address the technical challenges in 5G communication systems.

Conventional fully digital baseband signal processing schemes that require an individual radio frequency (RF) chain for each receive are impractical for the mmWave massive MIMO systems because of the high hardware complexity, power consumption and cost that such an architecture entails. Therefore, hybrid combining techniques, which need a significantly lower number of RF chains in comparison to the number of transmit/ receive antennas, have been shown to be well suited for mmWave MIMO systems [3]. In this context, the authors in [4] have analyzed the spectral efficiencies of both centralized and distributed mmWave massive MIMO systems with hybrid precoding. A few works in the existing literature [5]–[7] have proposed fusion rules based on linear filtering at the fusion center (FC) for massive MIMO wireless sensor networks (WSNs).

However, none of the works have proposed hybrid combining based fusion rules for mmWave massive MIMO WSNs. Therefore, this work considers a coherent multiple access channel (MAC)-based WSN, where several nodes simultaneously communicate with the FC equipped with a massive antenna array in the mmWave band. Each sensor node transmits a decision vector over one or more signaling intervals to convey its local decision to the FC. A low complexity fusion rule based on hybrid combining is determined for distributed detection in the mmWave massive MIMO WSN, incorporating also the probabilities of detection $(P_{D,k})$ and false alarm $(P_{F,k})$ of the local sensor decisions. Closed-form expressions are derived for the system level probabilities of detection and false alarm at the FC to analytically characterize the performance of the proposed detectors. Moreover, a deflection coefficient maximization based optimization framework is developed to obtain the optimal signaling matrix, which can further enhance the detection performance of the proposed scheme. Finally, simulation results are presented to demonstrate the detection performance of the proposed scheme.

II. System Model

Consider a mmWave massive MIMO WSN wherein K sensors are sensing a specific signal of interest. This framework can be modeled as a distributed binary hypothesis testing problem, where the null hypothesis $\mathcal{H}_0$ and the alternate hypothesis $\mathcal{H}_1$ indicate the absence and presence of the signal of interest, respectively. The WSN comprises of K single-antenna sensors which are simultaneously communicating with the FC over a flat fading coherent MAC. The FC is equipped with a massive antenna array of M antennas and N_{RF} radio frequency (RF) chains, such that $M \gg K$ and $N_{RF} = K$. Each RF chain can access all the M receive antennas at the FC. Depending on the local decision, the kth sensor, $1 \leq k \leq K$, transmits a decision vector $\mathbf{x}_k = [x_k(1), x_k(2), \ldots, x_k(N)]^T \in \mathbb{C}^{N\times 1}$ over N signaling intervals and it can be either $\mathbf{x}_k = \mathbf{u}_k$ or $\mathbf{x}_k = -\mathbf{u}_k$, indicating the presence or absence of the signal of interest, respectively. The probabilities of detection $P_{D,k}$ and false alarm $P_{F,k}$ of the kth sensor are defined as

$$\begin{aligned} P_{D,k} &= \Pr\left(\mathbf{x}_k = \mathbf{u}_k | \mathcal{H}_1\right), \\ P_{F,k} &= \Pr\left(\mathbf{x}_k = \mathbf{u}_k | \mathcal{H}_0\right). \end{aligned} \tag{1}$$

The received signal $\mathbf{y}(n) \in \mathbb{C}^{M\times 1}$ at the FC during the nth signaling instant can be expressed as

$$\mathbf{y}(n) = \sqrt{p_u}\mathbf{G}\mathbf{x}(n) + \mathbf{w}(n), \tag{2}$$

where $\mathbf{G} \in \mathbb{C}^{M\times K}$ represents the mmWave channel matrix between the FC and the K sensors, $\mathbf{x}(n) = [x_1(n), x_2(n), \ldots, x_K(n)] \in \mathbb{C}^{K\times 1}$ denotes the composite

transmitted signal vector comprising of symbols from all the K sensors and p_u is the average transmit power of each sensor. The vector $\mathbf{w}(n) \in \mathbb{C}^{M\times 1}$ denotes the complex Gaussian noise at the nth signaling interval with distribution as $\mathbf{w}(n) \sim \mathcal{CN}\left(0, \sigma_w^2 I_M\right)$. The channel vector $\mathbf{g}_k \in \mathbb{C}^{M\times 1}$ between the kth sensor and the FC is represented by $\mathbf{g}_k = \sqrt{\beta}_k \mathbf{h}_k$, where $\mathbf{h}_k$ and $\sqrt{\beta}_k$ denote the small-scale fading vector and large-scale fading coefficient between the kth sensor and the FC, respectively. The large-scale fading coefficient $\sqrt{\beta}_k$ accounts for the pathloss and log-normal shadowing effects, which is assumed to be constant over multiple coherence intervals and independent across m, $1 \leq m \leq M$. Employing the extended Saleh-Valenzuela (SV) model for mmWave channel modeling [8], the small-scale fading vector $\mathbf{h}_k$ can be characterized as

$$\mathbf{h}_k = \sqrt{\frac{M}{L_k}} \sum_{l=1}^{L_k} \alpha_k^l \mathbf{a}_r\left(\theta_k^l\right), \tag{3}$$

where $\alpha_k^l \sim \mathcal{CN}(0,1)$ and $\theta_k^l \in [0, 2\pi]$ represent the complex gain and angle of arrival corresponding to the lth path and the kth sensor, respectively. The parameter L_k denotes the number of propagation paths observed by the kth sensor and it follows the discrete uniform distribution, i.e., $L_k \sim \mathcal{DU}[1, L_m]$ with L_m as the maximum number of propagation paths. For a uniform linear array (ULA) configuration at the FC, the vector $\mathbf{a}_r\left(\theta_k^l\right) \in \mathbb{C}^{M\times 1}$ that corresponds to the receive array response vector of the kth sensor and the FC can be expressed as

$$\mathbf{a}_r\left(\theta_k^l\right) = \frac{1}{\sqrt{M}}\left[1, e^{jv\sin\left(\theta_k^l\right)}, \ldots, e^{jv(M-1)\sin\left(\theta_k^l\right)}\right]^T, \tag{4}$$

where $v = \frac{2\pi}{\lambda} d$, d is the spacing between the antenna elements and λ is the carrier wavelength. Therefore, the channel matrix $\mathbf{G}$ can be modeled as

$$\mathbf{G} = \mathbf{H}\mathbf{D}^{1/2}, \tag{5}$$

where $\mathbf{H} \in \mathbb{C}^{M\times K}$ is the small-scale fading matrix obtained using (3) and the diagonal matrix $\mathbf{D}$ is the large-scale fading matrix with β_k, $1 \leq k \leq K$, along its principal diagonal. Utilizing (2), the received signal $\mathbf{Y} \in \mathbb{C}^{M\times N}$ at the FC corresponding to the N composite transmitted vectors $\mathbf{x}(n)$, can be expressed as

$$\mathbf{Y} = \sqrt{p_u}\mathbf{G}\mathbf{X} + \mathbf{W}, \tag{6}$$

where $\mathbf{X} = [\mathbf{x}(1), \ldots, \mathbf{x}(N)] \in \mathbb{C}^{K\times N}$ denotes the transmitted signal matrix and $\mathbf{W} = [\mathbf{w}(1), \ldots, \mathbf{w}(N)] \in \mathbb{C}^{M\times N}$ is the noise matrix with its elements as i.i.d. random variables, i.e., $w_{i,j} \sim \mathcal{CN}(0, \sigma_w^2)$. The hybrid combining based fusion rule for the perfect CSI scenario is described next.

III. Fusion Rule and Hybrid Combiner

This section presents the fusion rule for the perfect CSI scenario at the FC. Based on the Neyman-Pearson (NP) criterion, the log likelihood ratio (LLR) test for the mmWave massive MIMO WSN system model in (6) can be formulated as

$$T\left(\mathbf{Y}\right) = \ln\left[\frac{p\left(\mathbf{Y}|\mathcal{H}_1\right)}{p\left(\mathbf{Y}|\mathcal{H}_0\right)}\right] \underset{\mathcal{H}_0}{\overset{\mathcal{H}_1}{\gtrless}} \gamma, \tag{7}$$

where γ is the detection threshold and $p\left(\mathbf{Y}|\mathcal{H}_1\right)$, $p\left(\mathbf{Y}|\mathcal{H}_0\right)$ represent the PDFs of $\mathbf{Y}$ under the hypotheses $\mathcal{H}_1$ and $\mathcal{H}_0$, respectively. The LLR test obtained after substituting the relevant PDFs in (7), can be expressed as

$$T(\mathbf{Y}) = \sum_{n=1}^{N} \ln\left[\frac{\sum_{\mathbf{x}(n)} \exp\left(-\frac{\|\mathbf{y}(n)-\sqrt{p_u}\mathbf{G}\mathbf{x}(n)\|^2}{\sigma_w^2}\right)\Pr(\mathbf{x}(n)|\mathcal{H}_1)}{\sum_{\mathbf{x}(n)} \exp\left(-\frac{\|\mathbf{y}(n)-\sqrt{p_u}\mathbf{G}\mathbf{x}(n)\|^2}{\sigma_w^2}\right)\Pr(\mathbf{x}(n)|\mathcal{H}_0)}\right].$$

However, the above test is numerically unstable and computationally complex because of the summation over 2^K exponential terms [5]. For a practically amenable implementation, a two step architecture is proposed to simplify the LLR test $T\left(\mathbf{Y}\right)$. In the first step, the received signal at the FC is processed by a hybrid combiner to recover the soft decisions of the individual sensors. The hybrid combiner comprises of an analog combiner $\mathbf{F}_{RF} \in \mathbb{C}^{M\times K}$ and a digital combiner $\mathbf{F}_{BB} \in \mathbb{C}^{K\times K}$. The analog combiner $\mathbf{F}_{RF}$ is obtained by concatenating the receive array response vectors of all the sensors corresponding to their maximum path gains and is given as

$$\mathbf{F}_{RF} = \left[\mathbf{a}_r\left(\theta_1^{l_1}\right), , \ldots, \mathbf{a}_r\left(\theta_K^{l_K}\right)\right], \tag{8}$$

where l_k denotes the path having the maximum path gain $\alpha_k^{l_k}$ and $\theta_k^{l_k}$, $1 \leq k \leq K$, represents the corresponding angle of arrival of the kth sensor. The matrix $\mathbf{F}_{BB}$ is obtained by utilizing the equivalent baseband channel matrix and is represented by $\mathbf{F}_{BB} = \mathbf{F}_{RF}^H \mathbf{G}$. In the second step, the processed sensor decisions are combined to obtain a final decision. After hybrid combining, the system model in (6) can be equivalently expressed as

$$\mathbf{Z} = \mathbf{F}_{\mathrm{BB}}^H \mathbf{F}_{\mathrm{RF}}^H \mathbf{Y} = \sqrt{p_u}\mathbf{F}_{\mathrm{BB}}^H \mathbf{F}_{\mathrm{RF}}^H \mathbf{G}\mathbf{X} + \mathbf{F}_{\mathrm{BB}}^H \mathbf{F}_{\mathrm{RF}}^H \mathbf{W}, \tag{9}$$

where $\mathbf{Z} = [\mathbf{z}(1), \ldots, \mathbf{z}(N)] \in \mathbb{C}^{K\times N}$ represents the output matrix obtained after hybrid combining. From the asymptotic orthogonality property of mmWave massive MIMO channels [9], it follows that

$$\mathbf{a}_r^H\left(\theta_k^{l_u}\right)\mathbf{a}_r\left(\theta_s^{l_v}\right) = \begin{cases} 1, & k = s \text{ and } u = v \\ 0, & k \neq s \text{ or } u \neq v \end{cases} \tag{10}$$

when M grows large and $L_k \ll M$, $\forall k$. Using the results described in (10), the hybrid combiner output vector $\mathbf{z}_k \in \mathbb{C}^{N\times 1}$ of the kth sensor, corresponding to the transmitted vector $\mathbf{x}_k = [x_k(1), \ldots, x_k(N)]^T \in \mathbb{C}^{N\times 1}$, can be equivalently expressed as

$$\mathbf{z}_k = \sqrt{p_u}\frac{M\beta_k}{L_k}|\alpha_k^{l_k}|^2 \mathbf{x}_k + \tilde{\mathbf{w}}_k, \tag{11}$$

where $\tilde{\mathbf{w}}_k = \sqrt{\frac{M\beta_k}{L_k}}\alpha_k^{l_k *}\left(\mathbf{a}_r^H\left(\theta_k^{l_k}\right)\mathbf{W}\right)^T \in \mathbb{C}^{N\times 1}$ is the equivalent noise vector with distribution as $\tilde{\mathbf{w}}_k \sim \mathcal{CN}\left(\mathbf{0}, \mathbf{C}_{\tilde{\mathbf{w}}_k}\right)$ and the covariance matrix $\mathbf{C}_{\tilde{\mathbf{w}}_k} \in \mathbb{C}^{N\times N}$ is defined as $\mathbf{C}_{\tilde{\mathbf{w}}_k} = M\sigma_w^2 d_k \mathbf{I}_N$, where $d_k \triangleq \frac{\beta_k}{L_k}\mathbb{E}\{|\alpha_k^{l_k}|^2\}$. The output vector $\mathbf{z}_k$ follows the complex Normal distribution, i.e., $\mathbf{z}_k \sim \mathcal{CN}\left(\sqrt{p_u}M d_k \mathbf{x}_k, \mathbf{C}_k\right)$ and the covariance matrix $\mathbf{C}_k \in \mathbb{C}^{N\times N}$ is defined as $\mathbf{C}_k = \frac{p_u M^2 \beta_k^2}{L_k^2}\mathbf{x}_k\mathbf{x}_k^H \mathrm{var}\{|\alpha_k^{l_k}|^2\} + \mathbf{C}_{\tilde{\mathbf{w}}_k}$. Therefore, the LLR based test statistic $T(\mathbf{Z})$ for distributed

detection in the mmWave massive MIMO WSN with perfect CSI can be determined as

$$T(\mathbf{Z}) = \ln\left[\frac{p(\mathbf{Z}|\mathcal{H}_1)}{p(\mathbf{Z}|\mathcal{H}_0)}\right] = \ln\left[\prod_{k=1}^{K}\frac{p(\mathbf{z}_k|\mathcal{H}_1)}{p(\mathbf{z}_k|\mathcal{H}_0)}\right]. \quad (12)$$

The above test can be simplified to the expression in (13). After substituting the relevant quantities, i.e., local sensor performance metrics from (1) and the conditional PDFs of $\mathbf{z}_k$ for $\mathbf{x}_k \in \{\mathbf{u}_k, -\mathbf{u}_k\}$, which are given as, $\phi(\mathbf{z}_k|\mathbf{x}_k{=}\mathbf{u}_k) \sim \mathcal{CN}\left(\sqrt{p_u}Md_k\mathbf{u}_k, \mathbf{C}_k\right)$ and $\phi(\mathbf{z}_k|\mathbf{x}_k{=}-\mathbf{u}_k) \sim \mathcal{CN}\left(-\sqrt{p_u}Md_k\mathbf{u}_k, \mathbf{C}_k\right)$, respectively, with $\mathbf{C}_k = \frac{p_u M^2\beta_k^2}{L_k^2}\mathbf{u}_k\mathbf{u}_k^H \text{var}\{|\alpha_k^{l_k}|^2\} + \mathbf{C}_{\tilde{\mathbf{w}}_k} = M\tilde{\mathbf{C}}_k$, the test statistic in (13) can be simplified as

$$T(\mathbf{Z}){=}\sum_{k=1}^{K}\ln\left[\frac{P_{D,k}{+}(1{-}P_{D,k})\exp\left(\frac{-4\sqrt{p_u}d_k}{\sigma_n^2}\Re(\mathbf{z}_k^H\tilde{\mathbf{C}}_k^{-1}\mathbf{u}_k)\right)}{P_{F,k}{+}(1{-}P_{F,k})\exp\left(\frac{-4\sqrt{p_u}d_k}{\sigma_n^2}\Re(\mathbf{z}_k^H\tilde{\mathbf{C}}_k^{-1}\mathbf{u}_k)\right)}\right],$$

where the symbol $\Re(.)$ represents the real part. For low SNR scenarios, the above test after employing the approximations $e^{-t} \approx (1-t)$ and $\ln(1+t) \approx t$, for sufficiently small values of t, reduces to

$$T(\mathbf{Z}) = \sum_{k=1}^{K} a_k d_k \Re\left(\mathbf{z}_k^H\tilde{\mathbf{C}}_k^{-1}\mathbf{u}_k\right) \underset{\mathcal{H}_0}{\overset{\mathcal{H}_1}{\gtrless}} \gamma', \quad (14)$$

where the constant a_k is defined as $a_k \triangleq (P_{D,k} - P_{F,k})$ for the kth sensor. The low SNR approximation based test statistic is suitable for practical scenarios because WSNs are generally resource constrained especially in terms of the transmit power. For identical local sensor performance metrics, i.e., $P_{D,k}{=}P_d$ and $P_{F,k}{=}P_f$, $\forall k$, the test statistic in (14) reduces to $T_{\text{I}}(\mathbf{Z}) = \sum_{k=1}^{K} d_k \Re(\mathbf{z}_k^H\tilde{\mathbf{C}}_k^{-1}\mathbf{u}_k)$. The analytical performance of the fusion rule in (14) is described below.

Theorem 1. *The probabilities of detection (P_D) and false alarm (P_{FA}) of the test statistic in* (14)*, for distributed detection in the mmWave massive MIMO WSN are given as*

$$P_D = Q\left(\frac{\gamma' - \mu_{T|\mathcal{H}_1}}{\sigma_{T|\mathcal{H}_1}}\right), \quad (15)$$

$$P_{FA} = Q\left(\frac{\gamma' - \mu_{T|\mathcal{H}_0}}{\sigma_{T|\mathcal{H}_0}}\right), \quad (16)$$

where $\mu_{T|\mathcal{H}_0}, \mu_{T|\mathcal{H}_1}, \sigma^2_{T|\mathcal{H}_0}$ and $\sigma^2_{T|\mathcal{H}_1}$ denote the mean and variance of the null and alternative hypotheses, respectively and are given as

$$\mu_{T|\mathcal{H}_0} = \sum_{k=1}^{K}\sqrt{p_u}Ma_kc_kd_k^2\|\mathbf{u}_k\|^2_{\tilde{\mathbf{C}}_k^{-1}}, \quad (17)$$

$$\mu_{T|\mathcal{H}_1} = \sum_{k=1}^{K}\sqrt{p_u}Ma_kb_kd_k^2\|\mathbf{u}_k\|^2_{\tilde{\mathbf{C}}_k^{-1}}, \quad (18)$$

$$\sigma^2_{T|\mathcal{H}_0} = \sum_{k=1}^{K}Md_k^2a_k^2\left(Mp_u\xi_k + \frac{\sigma_w^2}{2}d_k(\mathbf{u}_k^H\tilde{\mathbf{C}}_k^{-2}\mathbf{u}_k)\right), \quad (19)$$

$$\sigma^2_{T|\mathcal{H}_1} = \sum_{k=1}^{K}Md_k^2a_k^2\left(Mp_u\zeta_k + \frac{\sigma_w^2}{2}d_k(\mathbf{u}_k^H\tilde{\mathbf{C}}_k^{-2}\mathbf{u}_k)\right), \quad (20)$$

with $b_k = (2P_{D,k}-1)$, $c_k = (2P_{F,k}-1)$, $\xi_k = \left(\frac{\beta_k^2}{L_k^2}\mathbb{E}\{|\alpha_k^{l_k}|^4\} - d_k^2c_k^2\right)\left(\mathbf{u}_k^H\tilde{\mathbf{C}}_k^{-1}\mathbf{u}_k\right)^2$ *and* $\zeta_k = \left(\frac{\beta_k^2}{L_k^2}\mathbb{E}\{|\alpha_k^{l_k}|^4\} - d_k^2b_k^2\right)\left(\mathbf{u}_k^H\tilde{\mathbf{C}}_k^{-1}\mathbf{u}_k\right)^2$.

Proof. See Appendix A. □

IV. Signaling Matrices

This section develops the optimization framework to obtain the transmit signal matrix $\mathbf{X} = [\mathbf{x}_1, \mathbf{x}_2, \ldots, \mathbf{x}_K]^T \in \mathbb{C}^{K\times N}$, to further enhance the performance of the proposed detector for a mmWave massive MIMO WSN. The equivalent vector $\mathbf{x} \in \mathbb{C}^{KN\times 1}$, obtained by stacking the transmit vectors $\mathbf{x}_1, \mathbf{x}_2, \ldots, \mathbf{x}_K$, be defined as $\mathbf{x} = \text{vec}\left(\mathbf{X}^T\right) = [\mathbf{x}_1^T, \mathbf{x}_2^T, \ldots, \mathbf{x}_K^T]^T$ where $\mathbf{x}_k \in \{\mathbf{u}_k, -\mathbf{u}_k\}$, $\forall K$. The transmit signal matrix, which maximizes the detection performance, can be obtained by maximizing the deflection coefficient $d^2(\mathbf{u})$ for $\mathbf{u} = \text{vec}\left(\mathbf{U}^T\right)$ [10], defined as

$$d^2(\mathbf{u}) = \frac{\left(\mu_{T|\mathcal{H}_1} - \mu_{T|\mathcal{H}_0}\right)^2}{\sigma^2_{T|\mathcal{H}_0}}. \quad (21)$$

Substituting the expressions for $\mu_{T|\mathcal{H}_0}$, $\mu_{T|\mathcal{H}_1}$, $\sigma^2_{T|\mathcal{H}_0}$ from Theorem 1 in (21), the deflection coefficient $d^2(\mathbf{u})$ can be derived as

$$d^2(\mathbf{u}) = \frac{\left(\sum_{k=1}^{K}\sqrt{p_u}Md_k^2a_k(b_k-c_k)\|\mathbf{u}_k\|^2_{\tilde{\mathbf{C}}_k^{-1}}\right)^2}{\sum_{k=1}^{K}Md_k^2a_k^2\left(Mp_u\xi_k + \frac{\sigma_w^2}{2}d_k(\mathbf{u}_k^H\tilde{\mathbf{C}}_k^{-2}\mathbf{u}_k)\right)}$$
$$\approx \frac{(\mathbf{u}^H\mathbf{\Gamma}_N\mathbf{u})^2}{(\mathbf{u}^H\mathbf{\Psi}_N\mathbf{u})^2 + \mathbf{u}^H\mathbf{\Theta}_N\mathbf{u}}, \quad (22)$$

where $\mathbf{\Gamma}_N \in \mathbb{C}^{KN\times KN}$, $\mathbf{\Psi}_N \in \mathbb{C}^{KN\times KN}$ and $\mathbf{\Theta}_N \in \mathbb{C}^{KN\times KN}$ represent the block diagonal matrices such that their principal diagonal matrices are defined as $[\mathbf{\Gamma}_N]_{k,k} = \mathbf{\Gamma}_{k,k}\tilde{\mathbf{C}}_k^{-1}$, $[\mathbf{\Psi}_N]_{k,k} = \mathbf{\Psi}_{k,k}\tilde{\mathbf{C}}_k^{-1}$ and $[\mathbf{\Theta}_N]_{k,k} = \mathbf{\Theta}_{k,k}\tilde{\mathbf{C}}_k^{-2}$, respectively. The matrices $\mathbf{\Gamma} \in \mathbb{C}^{K\times K}$, $\mathbf{\Psi} \in \mathbb{C}^{K\times K}$ and $\mathbf{\Theta} \in \mathbb{C}^{K\times K}$ are diagonal matrices and their principal diagonal elements are defined as

$$[\mathbf{\Gamma}]_{k,k} = \sqrt{p_u}Md_k^2a_k(b_k-c_k), [\mathbf{\Theta}]_{k,k} = \frac{\sigma_w^2}{2}Md_k^3a_k^2,$$
$$[\mathbf{\Psi}]_{k,k} = \sqrt{p_u}Md_ka_k\sqrt{\frac{\beta_k^2}{L_k^2}\mathbb{E}\{|\alpha_k^{l_k}|^4\} - c_k^2d_k^2}. \quad (23)$$

The direct maximization of the deflection coefficient in (22) is difficult as the expression in (22) is non-convex. For a tractable solution, the optimization objective can be modified as

$$\text{max. } \frac{\mathbf{u}^H\left(\mathbf{\Gamma}_N\mathbf{u}\mathbf{u}^H\mathbf{\Gamma}_N\right)\mathbf{u}}{\mathbf{u}^H\left(\mathbf{\Psi}_N\mathbf{u}\mathbf{u}^H\mathbf{\Psi}_N + \mathbf{\Theta}_N\right)\mathbf{u}} = \text{max. } \frac{\mathbf{u}^H\mathbf{\Xi}\mathbf{u}}{\mathbf{u}^H\mathbf{\Omega}\mathbf{u}}, \quad (24)$$

where $\mathbf{\Xi} = \mathbf{\Gamma}_N\mathbf{u}\mathbf{u}^H\mathbf{\Gamma}_N$, $\mathbf{\Omega} = \mathbf{\Psi}_N\mathbf{u}\mathbf{u}^H\mathbf{\Psi}_N + \mathbf{\Theta}_N$. The objective function in (24) can be further simplified, similar to the two-way partitioning problem, [11] as

$$\text{max. } \frac{\mathbf{u}^H\mathbf{\Xi}\mathbf{u}}{\mathbf{u}^H\mathbf{\Omega}^{1/2}\mathbf{\Omega}^{1/2}\mathbf{u}} = \text{max. } \frac{\mathbf{s}^H\mathbf{\Omega}^{-1/2}\mathbf{\Xi}\mathbf{\Omega}^{-1/2}\mathbf{s}}{\mathbf{s}^H\mathbf{s}}$$
$$= \text{max. } \frac{\mathbf{s}^H\mathbf{Q}\mathbf{s}}{\mathbf{s}^H\mathbf{s}}, \quad (25)$$

$$T(\mathbf{Z})=\sum_{k=1}^{K}\ln\left[\frac{\phi(\mathbf{z}_k|\mathbf{x}_k=\mathbf{u}_k)\Pr(\mathbf{x}_k=\mathbf{u}_k|\mathcal{H}_1)+\phi(\mathbf{z}_k|\mathbf{x}_k=-\mathbf{u}_k)\Pr(\mathbf{x}_k=-\mathbf{u}_k|\mathcal{H}_1)}{\phi(\mathbf{z}_k|\mathbf{x}_k=\mathbf{u}_k)\Pr(\mathbf{x}_k=\mathbf{u}_k|\mathcal{H}_0)+\phi(\mathbf{z}_k|\mathbf{x}_k=-\mathbf{u}_k)\Pr(\mathbf{x}_k=-\mathbf{u}_k|\mathcal{H}_0)}\right] \tag{13}$$

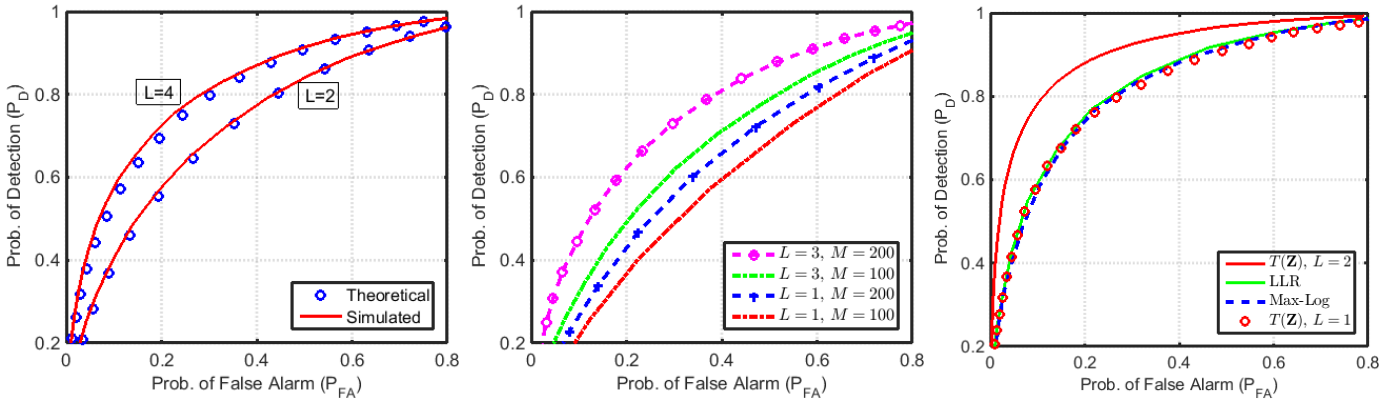

(a) (b) (c)

Fig. 1. Receiver operating characteristic (ROC) plot for comparing (a) theoretical and simulated performance of the detector in (14) with $K = 12$ sensors, $M = 250$ antennas, $L \in \{2, 4\}$ and SNR $p_u = -18$ dB. (b) proposed detector in (14) for $M \in \{100, 200\}$ antennas, $K = 12$ sensors, $L \in \{1, 3\}$ and at SNR $p_u = -18$ dB. (c) Max-Log and LLR detectors with the proposed detector (14) for $M = 250$ antennas, $K = 12$ sensors, $L = 1$ and at SNR $p_u = -18$ dB.

where $\mathbf{Q} = \mathbf{\Omega}^{-1/2}\mathbf{\Xi}\mathbf{\Omega}^{-1/2}$ and $\mathbf{s} = \mathbf{\Omega}^{1/2}\mathbf{u}$. Let $\mathbf{u}$ be initialized as $\mathbf{u}^{(0)} = \text{vec}\left(\left(\mathbf{U}^{(0)}\right)^T\right)$, where the matrix $\mathbf{U}^{(0)}$ represents a semi-unitary matrix at the 0th iteration. The iterative optimization problem during the ith iteration to derive the signaling matrix that further enhances the detection performance of the proposed detector for a mmWave massive MIMO WSN is discussed next.

Theorem 2. *The signaling matrix $\mathbf{U}^{(i)}$ during the ith iteration for distributed detection in mmWave massive MIMO WSN is given as $\mathbf{U}^{(i)} = \left(vec^{-1}\left(\left(\mathbf{\Omega}^{(i-1)}\right)^{-1/2}\mathbf{s}^{(i)}\right)\right)^T$, where $\mathbf{s}^{(i)}$ is the solution of the optimization problem below*

$$\max_{\mathbf{s}^{(i)}} \ \frac{\mathbf{s}^{(i)H}\mathbf{Q}^{(i-1)}\mathbf{s}^{(i)}}{\mathbf{s}^{(i)H}\mathbf{s}^{(i)}}, \tag{26}$$

where $\mathbf{Q}^{(i-1)} = \left(\mathbf{\Omega}^{(i-1)}\right)^{-1/2}\mathbf{\Xi}^{(i-1)}\left(\mathbf{\Omega}^{(i-1)}\right)^{-1/2}$ and $\mathbf{s}^{(i)} = \left(\mathbf{\Omega}^{(i-1)}\right)^{1/2}\mathbf{u}^{(i)}$. The matrices $\mathbf{\Xi}^{(i-1)}, \mathbf{\Omega}^{(i-1)}$ are obtained by substituting $\mathbf{u}^{(i-1)}$ in lieu of $\mathbf{u}$ in (24)*.*

The solution $\mathbf{u}^{(i)}$ is obtained [6] by solving the optimization problem in (26) and is given as $\mathbf{u}^{(i)} = \kappa\left(\mathbf{\Omega}^{(i-1)}\right)^{-1/2}\boldsymbol{\nu}^{(i-1)}$, where $\boldsymbol{\nu}^{(i-1)}$ denotes the eigenvector corresponding to the maximum eigenvalue of the matrix $\mathbf{Q}^{(i-1)}$ and κ is the total power of $\mathbf{u}^{(i)}$.

V. Simulation Results

This section demonstrates the detection performance of the proposed detector in (14) for the mmWave massive MIMO WSN and its comparison with other detectors, namely, the Max-Log and the LLR, with the help of simulation results. A total of $K = 12$ single-antenna sensors are assumed to be randomly placed in an annular region around the FC with minimum and maximum distances as $r_c = 1$ m and $r = 100$ m, respectively. The local probabilities of detection ($P_{D,k}$) and false alarm ($P_{F,k}$) are assumed to be uniformly distributed in the intervals [0.95,0.40] and [0.01,0.12], respectively [6]. The large-scale fading coefficients are defined as $\beta_k = \nu_k / (r_k/r_c)^{\delta}$ [12], $\forall k$, where r_k is the distance of the kth sensor from the FC, ν_k is a log-normal random variable, i.e, $10\log_{10}\nu_k \sim \mathcal{N}(\mu, \sigma^2)$ and δ denotes the path-loss exponent. The parameters are chosen as μ = 4 dB, σ = 2 dB, δ = 2, carrier frequency f_c = 28 GHz, inter-antenna spacing d at the FC = $\frac{\lambda}{2}$, maximum number of propagation paths L_m = 10, noise variance σ_w^2 = 1, SNR p_u = -18 dB and number of antennas at the FC M = 250.

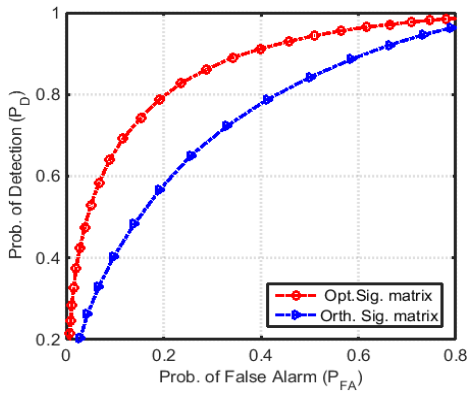

Fig. 2. ROC plot for comparing detector $T(\mathbf{Z})$ with orthogonal and optimized signaling matrix obtained in Section IV, for a WSN with $K = 12$ sensors, $L = 2$, $M = 250$ and SNR $p_u = -18$ dB.

Fig. 1a plots the probability of detection (P_D) versus probability of false alarm (P_{FA}) for varying $L = \{2, 4\}$. It is evident

from the figure that the analytical results obtained in Theorem 1 are in close agreement with the simulated plots, validating our derived results. Fig. 1b illustrates the effect of varying the signaling intervals of the decision vector $L = \{1, 3\}$ and the number of antennas $M = \{100, 200\}$ at the FC. It can be observed that the detection performance improves as the number of signaling intervals and antennas increases, thus confirming the advantage of using massive MIMO technology. Fig. 1c shows the comparison of the receiver operating characteristic (ROC) of the proposed scheme with the detectors, namely, the LLR and the Max-Log. It can be inferred from the figure that the proposed detector has similar performance as that of the Max-Log detector and the LLR test of $\mathbf{Z}$, for the low SNR regime. Finally, Fig. 2 explores the aspect of signaling matrix optimization to further improve the detection performance. An improved performance is observed by utilizing the deflection-coefficient maximization based signaling matrix, obtained in Section IV, for $L = 2$.

VI. Conclusion

This paper investigated the hybrid combining based detection rule for distributed detection in a mmWave massive MIMO WSN. The analysis incorporates the probability of error of the local sensor decisions. Further, the closed-form expressions of probabilities of detection P_D and false alarm P_{FA} are determined to characterize the system performance. Simulation results are demonstrated to compare the performance of the proposed detector with the LLR and Max-Log detectors. A deflection coefficient maximization based optimization framework is also developed to obtain a signaling matrix, which can enhance the detection performance. Simulation results demonstrated the improved performance of the proposed schemes in comparison to the existing ones.

Appendix A
Proof of Theorem 1

The mean corresponding to the hypothesis $\mathcal{H}_1$ for the detection rule in (14) is given as $\mu_{T|\mathcal{H}_1} = \sum_{k=1}^{K} \mu_1$, where μ_1 can be determined as

$$\begin{aligned}
\mu_1 =& a_k d_k \Re\left(\mathbb{E}\{\mathbf{z}_k^H \tilde{\mathbf{C}}_k^{-1}\mathbf{u}_k|\mathcal{H}_1\}\right)\\
=& a_k d_k \Re\left(\sqrt{p_u}M\left(\frac{\beta_k}{L_k}\mathbb{E}\{|\alpha_k^{l_k}|^2\}\right)\mathbb{E}\{\mathbf{x}_k^H|\mathcal{H}_1\}\tilde{\mathbf{C}}_k^{-1}\mathbf{u}_k\right)\\
=& a_k d_k \Re\big(\sqrt{p_u}M d_k(\mathbf{u}_k^H \Pr(\mathbf{x}_k = \mathbf{u}_k|\mathcal{H}_1)\\
&- \mathbf{u}_k^H \Pr(\mathbf{x}_k = -\mathbf{u}_k|\mathcal{H}_1))\tilde{\mathbf{C}}_k^{-1}\mathbf{u}_k\big)\\
=& a_k d_k \Re\big(\sqrt{p_u}M d_k(\mathbf{u}_k^H P_{D,k} - \mathbf{u}_k^H(1-P_{D,k}))\tilde{\mathbf{C}}_k^{-1}\mathbf{u}_k\big)\\
=& \sqrt{p_u}M a_k b_k d_k^2(\mathbf{u}_k^H\tilde{\mathbf{C}}_k^{-1}\mathbf{u}_k), \qquad (27)
\end{aligned}$$

which reduces to the expression in (18). On similar lines, the mean for hypothesis $\mathcal{H}_0$ in (17) can be derived. The variance of the test statistic $T(\mathbf{Z})$ corresponding to hypothesis $\mathcal{H}_1$, can be expressed as

$$\sigma^2_{T|\mathcal{H}_1} = \mathbb{E}\{T^2(\mathbf{Z})|\mathcal{H}_1\} - \left(\mathbb{E}\{T(\mathbf{Z})|\mathcal{H}_1\}\right)^2, \qquad (28)$$

The first quantity in (28), i.e., $\epsilon = \mathbb{E}\{T^2(\mathbf{Z})|\mathcal{H}_1\} = \mathbb{E}\big\{\big(\sum_{k=1}^{K} a_k d_k \Re\{\mathbf{z}_k^H\tilde{\mathbf{C}}_k^{-1}\mathbf{u}_k\}\big)^2|\mathcal{H}_1\big\}$, can be simplified as

$$\epsilon = \mathbb{E}\Big\{\Big(\sum_{k=1}^{K} a_k d_k \Re\Big\{\Big(\sqrt{p_u}M\frac{\beta_k}{L_k}|\alpha_k^{l_k}|^2\mathbf{x}_k^H + \tilde{\mathbf{w}}_k^H\Big)\tilde{\mathbf{C}}_k^{-1}\mathbf{u}_k\Big\}\Big)^2\Big|\mathcal{H}_1\Big\}$$

which further reduces to

$$\epsilon = \sum_{k=1}^{K}\sum_{j=1,j\neq k}^{K} p_u M^2 a_k a_j d_j^2 d_k^2 b_k b_j \|\mathbf{u}_k\|^2_{\tilde{\mathbf{C}}_k^{-1}}\|\mathbf{u}_j\|^2_{\tilde{\mathbf{C}}_j^{-1}} +$$
$$\sum_{k=1}^{K} p_u M^2 a_k^2 d_k^2 \frac{\beta_k^2}{L_k^2}\mathbb{E}\{|\alpha_k^{l_k}|^4\}\|\mathbf{u}_k\|^2_{\tilde{\mathbf{C}}_k^{-1}} + \sum_{k=1}^{K}\frac{\sigma_w^2}{2}M a_k^2 d_k^3\|\tilde{\mathbf{C}}_k^{-1}\mathbf{u}_k\|^2$$

and the terms $\mathbb{E}\{|\alpha_k^{i_k}|^2\}$ and $\mathbb{E}\{|\alpha_k^{i_k}|^4\}$ are defined as

$$\mathbb{E}\{|\alpha_k^{i_k}|^2\} = \int_0^\infty m L_k(1-e^{-m})^{L_k-1}e^{-m}dm = \sum_{t=1}^{L_k}\frac{1}{t}\binom{L_k}{t}(-1)^{t-1}$$

$$\mathbb{E}\{|\alpha_k^{i_k}|^4\} = \int_0^\infty m^2 L_k(1-e^{-m})^{L_k-1}e^{-m}dm = \sum_{t=1}^{L_k}\frac{2}{t}\binom{L_k}{t}(-1)^{t-1}$$

The variance $\sigma^2_{T|\mathcal{H}_1}$ in (20) can be obtained, using the above expressions (18) and (28).

References

[1] T. Rappaport, R. Heath, R. Daniels, and J. Murdock, *Millimeter wave wireless communications*. Prentice Hall, 2015, includes bibliographical references (pages 585-651) and index.

[2] T. S. Rappaport, S. Sun, R. Mayzus, H. Zhao, Y. Azar, K. Wang, G. N. Wong, J. K. Schulz, M. Samimi, and F. Gutierrez, "Millimeter Wave Mobile Communications for 5G Cellular: It Will Work!" *IEEE Access*, vol. 1, pp. 335–349, 2013.

[3] R. W. Heath, N. Gonzlez-Prelcic, S. Rangan, W. Roh, and A. M. Sayeed, "An Overview of Signal Processing Techniques for Millimeter Wave MIMO Systems," *IEEE J. Sel. Topics Signal Process.*, vol. 10, no. 3, pp. 436–453, April 2016.

[4] J. Li, D. Yue, and Y. Sun, "Performance Analysis of Millimeter Wave Massive MIMO Systems in Centralized and Distributed Schemes," *IEEE Access*, vol. 6, pp. 75 482–75 494, 2018.

[5] D. Ciuonzo and P. Salvo Rossi and S. Dey, "Massive MIMO Channel-Aware Decision Fusion," *IEEE Trans. Signal Process.*, vol. 63, no. 3, pp. 604–619, Feb. 2015.

[6] A. Chawla, A. Patel, A. K. Jagannatham, and P. K. Varshney, "Distributed Detection in Massive MIMO Wireless Sensor Networks under Perfect and Imperfect CSI," *IEEE Trans. Signal Process.*, vol. 56, no. 9, pp. 4124–4140, Jun. 2019.

[7] ——, "Robust Distributed Detection in Massive MIMO Wireless Sensor Networks Under CSI Uncertainty," in *IEEE 88th Veh. Technol. Conf.*, Aug. 2018, pp. 1–5.

[8] A. A. M. Saleh and R. Valenzuela, "A Statistical Model for Indoor Multipath Propagation," *IEEE J. Sel. Areas Commun.*, vol. 5, no. 2, pp. 128–137, Feb. 1987.

[9] S. Zhou, W. Xu, H. Zhang, and X. You, "Hybrid precoding for millimeter wave massive MIMO with analog combining," in *2017 9th Int. Conf. Wireless Commun. Signal Process. (WCSP)*, Oct. 2017, pp. 1–5.

[10] S. M. Kay, *Fundamentals of Statistical Signal Processing, Volume 2: Detection Theory*. New Jersey: Prentice-Hall Inc, 1993.

[11] S. Boyd and L. Vandenberghe, *Convex Optimization*. New York, NY, USA: Cambridge University Press, 2004.

[12] H. Q. Ngo, E. G. Larsson, and T. L. Marzetta, "Energy and Spectral Efficiency of Very Large Multiuser MIMO Systems," *IEEE Trans. Commun.*, vol. 61, no. 4, pp. 1436–1449, Apr. 2013.